

## Orbital-spin order and the origin of structural distortion in $\text{MgTi}_2\text{O}_4$

S. Leoni,<sup>1</sup> A. N. Yaresko,<sup>2</sup> N. Perkins,<sup>3</sup> H. Rosner,<sup>1</sup> and L. Craco<sup>1</sup>

<sup>1</sup>Max-Planck-Institut für Chemische Physik fester Stoffe, D-01187 Dresden, Germany

<sup>2</sup>Max-Planck-Institut für Festkörperforschung, Heisenbergstraße 1, D-70569 Stuttgart, Germany

<sup>3</sup>University of Wisconsin-Madison, 1150 University Avenue, Madison, Wisconsin 53706-1390, USA  
(Received 27 June 2008; revised manuscript received 15 July 2008; published 11 September 2008)

We analyze electronic, magnetic, and structural properties of the spinel compound  $\text{MgTi}_2\text{O}_4$  using the local-density approximation+ $U$  method. We show how  $\text{MgTi}_2\text{O}_4$  undergoes to a canted orbital-spin ordered state, where charge, spin, and orbital degrees of freedom are frozen in a geometrically frustrated network by electron interactions. In our picture orbital order stabilizes the magnetic ground state and controls the degree of structural distortions. The latter is dynamically derived from the cubic structure in the correlated LDA+ $U$  potential. Our ground-state theory provides a consistent picture for the dimerized phase of  $\text{MgTi}_2\text{O}_4$ , and might be applicable to frustrated materials in general.

DOI: [10.1103/PhysRevB.78.125105](https://doi.org/10.1103/PhysRevB.78.125105)

PACS number(s): 71.30.+h, 72.80.Ga, 61.66.Fn, 71.15.Mb

### I. INTRODUCTION

Over the last few years, a lot of progress has been achieved in the study of transition-metal oxides on frustrated lattices. Interest in these systems stems from the richness of their novel properties: the unexpected variety of ordered states and transitions between them, and the complexity of the underlying physics. Transition-metal oxide (TMO) spinels  $\text{AB}_2\text{O}_4$ , with magnetic B ions forming a pyrochlore lattice, give the unique possibility to explore how the natural tendency of correlated systems to develop magnetic, orbital, and charge order is affected by geometrical frustration.<sup>1,2</sup> The best studied example of TMO spinels, and historically the first one, is magnetite  $\text{Fe}_3\text{O}_4$ , which shows a high Curie temperature and undergoes the Verwey transition at  $T_V \approx 120$  K.<sup>2</sup>

Recently, B-spinel  $\text{MgTi}_2\text{O}_4$ , which is characterized by a pyrochlore lattice of  $\text{Ti}^{3+}$  magnetic ions with one single electron in the  $t_{2g}$  manifold, has attracted much attention due to a very peculiar phase transition from a metallic to a spin-singlet insulating phase near  $T_C \approx 260$  K.<sup>3</sup> The signature of the insulating state is the optical gap ( $\approx 0.25$  eV at  $T = 10$  K) observed in optical conductivity spectra.<sup>4</sup> Taken together, dc resistivity<sup>3,5</sup> and optical<sup>4,6</sup> measurements consistently indicate that  $\text{MgTi}_2\text{O}_4$  undergoes a sharp metal-insulator transition (MIT) with no sign of Drude weight at low frequencies below  $T_C$ . The MIT is accompanied by a structural transition from cubic to tetragonal symmetry, with a concomitant drop of the magnetic susceptibility and a resistivity jump below  $T_C$ . Neutron diffraction and x-ray measurements<sup>7</sup> indicate spin dimerization: Ti-Ti dimers are formed in a helical pattern in the spin-singlet state. Further structural refinements<sup>8</sup> reveal that Ti ions move away from the center of the  $\text{TiO}_6$  octahedron. In the low- $T$  phase two out of six Ti-Ti bonds get closer, suggesting the formation of chemical dimers. These findings have suggested a removal of the pyrochlore degeneracy by a one-dimensional (1D) helical dimerization of the spin pattern, with spin singlets (dimers) located at short bonds.

There were several theoretical attempts to understand the nature of spin dimerization and the origin of the MIT in

$\text{MgTi}_2\text{O}_4$ . Khomskii and Mizokawa<sup>9</sup> assumed that the system is close to an itinerant state and explained the formation of the nonmagnetic spin-singlet state by exploiting the concept of an *orbitally driven Peierls state*, leading to the formation of quasi-1D bands. In this case, the magnetic changes across the structural transition in  $\text{MgTi}_2\text{O}_4$  can be understood within the picture of 1D Peierls transition driven by the ordering (Fig. 1) of the  $d_{xz}$  and  $d_{yz}$  orbitals. This picture is consistent with B3LYP functional [generalized gradient approximation (GGA)] calculations<sup>7</sup> for the tetragonal phase of  $\text{MgTi}_2\text{O}_4$ , showing that the  $xz$  and  $yz$  orbitals are occupied while the  $xy$  states are pushed to high energies.

Another approach is based on the assumption that the low-temperature tetragonal phase of  $\text{MgTi}_2\text{O}_4$  is Mott insulator.<sup>10</sup> In this case, the ground state of  $\text{MgTi}_2\text{O}_4$  can be found by studying an effective low-energy spin-orbital superexchange Hamiltonian. It was shown in Ref. 10 that the orbital degrees of freedom in  $\text{MgTi}_2\text{O}_4$  modulates the spin exchange couplings, providing an explanation for the helical spin-singlet pattern observed in Ref. 7. It appears that the minimum energy configuration corresponds to such an orbital ordering for which the maximum number of spin-singlet dimers is formed. However, there are various dimer coverings of the pyrochlore lattice which have the same energy. As in spin-Peierls systems, the increase in magnetic energy gain can be achieved by the shortening of bonds, where dimers are situated. Therefore, each type of dimer coverings corresponding to a particular orbital ordering induces a different distortion of the lattice, which costs a different elastic energy. The ground state is chosen simply by finding a minimum energy state, which in case of  $\text{MgTi}_2\text{O}_4$  corresponds to the minimal enlargement of the unit cell.

However, no theoretical studies have been yet performed in order to understand the origin of the MIT and the formation of the spin-singlet state. Is it the intrinsic lower dimensionality of  $\text{MgTi}_2\text{O}_4$  that causes the formation of the spin-singlet state, or is the driving mechanism of different type?

In this work, in order to address these questions, we perform a quantitative investigation of the band structure of  $\text{MgTi}_2\text{O}_4$ . Using local- (spin) density approximation plus Hubbard  $U$ ,  $L(S)DA+U$ , approach,<sup>11</sup> we show how an explicit incorporation of electronic correlations allows for a

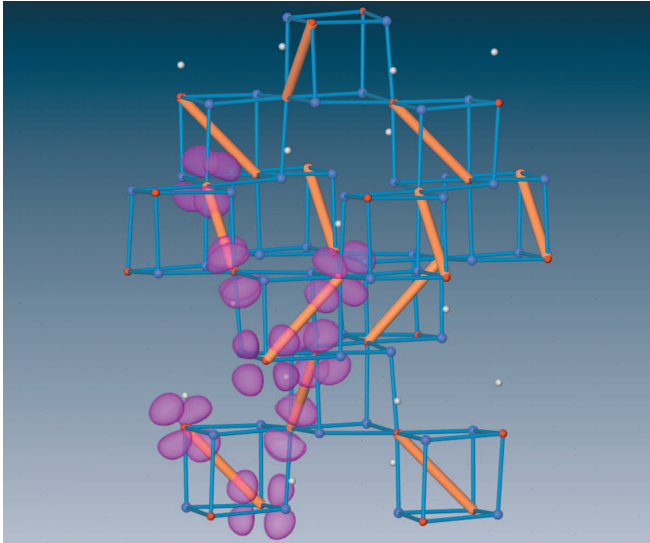


FIG. 1. (Color) Orbital order in the tetragonal crystal structure of  $\text{MgTi}_2\text{O}_4$  within the LDA+ $U$  framework ( $U=3$  eV). The electron density of the most populated  $t_{2g}$  orbital is plotted. Lattice constants are taken from Ref. 7. The orange bonds represent the shortest bonds in the distorted structure, and the corresponding atoms are displayed in red (Ti), blue (O), and white (Mg).

realistic description of the insulating ground state of  $\text{MgTi}_2\text{O}_4$ . Our results reveal that electronic correlations are fundamental in stabilizing the dimerized ground state of  $\text{MgTi}_2\text{O}_4$ . We show that MIT is driven by correlation (via LDA+ $U$ ) induced orbital order (OO) rearrangement. Therein,  $U$  controls band splitting toward an orbital-insulating state *without* full orbital polarization (OP). In our picture OO stabilizes the spin-singlet ground state, which in turn controls the degree of structural distortions. This finding is consistent with the superexchange spin-orbital description.<sup>10</sup> The opening of the electronic band gap is understood in terms of an orbital-selective MIT (Ref. 12) on a quasi-1D network.

## II. RESULTS AND DISCUSSION

To elucidate the interplay between spin, orbital, and charge degrees of freedom in  $\text{MgTi}_2\text{O}_4$  we perform *correlated* scalar-relativistic band-structure calculations using local- (spin) density approximation plus Hubbard  $U$ ,  $L(S)DA+U$ , approach.<sup>11</sup> We employ the linear muffin-tin orbital (LMTO) scheme in the atomic sphere approximation, with combined correction terms.<sup>13</sup>

Self-consistency is reached by performing calculations on a  $12 \times 12 \times 10$   $\mathbf{k}$ -mesh for the Brillouin-zone integration. Experimental atomic positions<sup>7</sup> for the tetragonal ( $P4_12_12$ ) low- $T$  phase were used in the calculations. The radii of the atomic spheres were chosen as  $r=2.4789$  (Mg),  $r=2.0022$ ,  $2.0106$  (O1, O2), and  $r=2.5857$  (Ti) a.u. in order to minimize their overlap.

Our results for the paramagnetic (LDA+ $U$ ) phase of  $\text{MgTi}_2\text{O}_4$  are presented in Fig. 2. Therein the evolution of the  $3d^1$  correlated density of states (DOS) is shown. In cubic

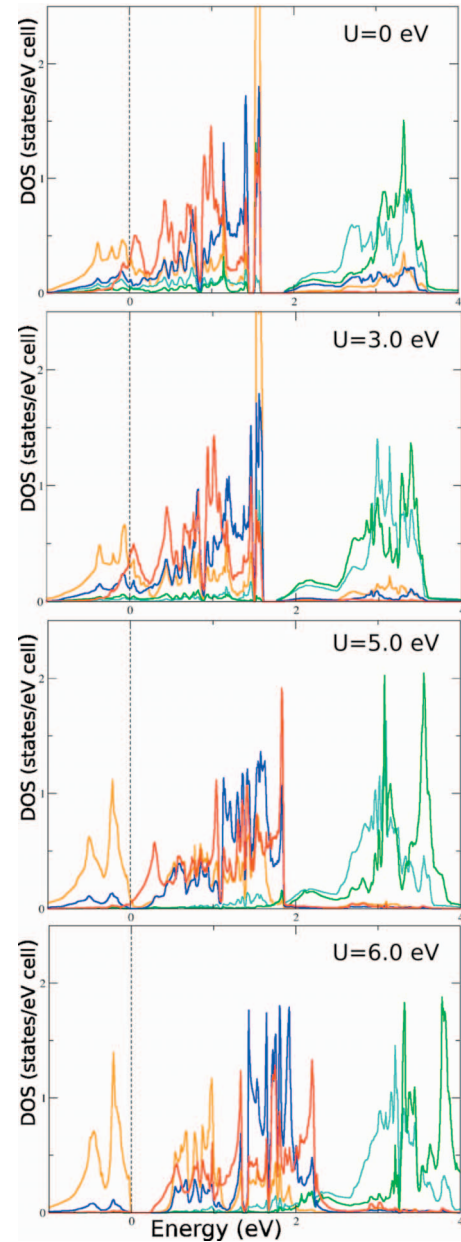


FIG. 2. (Color) LDA+ $U$  orbital resolved DOS for the tetragonal ( $P4_12_12$ ) (Ref. 7) phase of  $\text{MgTi}_2\text{O}_4$ :  $U=0$  eV (top left),  $U=3$  eV (top right),  $U=5$  eV (bottom left), and  $U=6$  eV (bottom right). Notice the orbital-selective nature of the correlation-induced metal-insulator transition between  $5 \text{ eV} < U < 6 \text{ eV}$  solutions.

spinel oxides the  $d$ -electron orbital sector splits into the low-energy  $t_{2g}$  and high-energy  $e_g$  orbitals. Below we will denote the  $t_{2g}$  orbitals in the tetragonal phase as  $XY$ ,  $XZ$ , and  $YZ$ , which differ from the  $d_{xy}$ ,  $d_{yz}$  and  $d_{zx}$  in the cubic phase (see details in Ref. 14). The corresponding DOS are plotted in red ( $XY$ ), orange ( $XZ$ ), and blue ( $YZ$ ) in Fig. 2. The DOS with dominant  $e_g$  contribution are shown by green and cyan curves. Due to partial oxygen relaxation, the crystal field has also a small trigonal component, which further splits the  $t_{2g}$  manifold into  $a_{1g}$  and  $e'_g$  sectors.<sup>15</sup> We note that the  $XZ$  orbitals directed along one of the short Ti-Ti bonds can only be formed as a linear combination of the  $a_{1g}$  and  $e'_g$  orbitals.

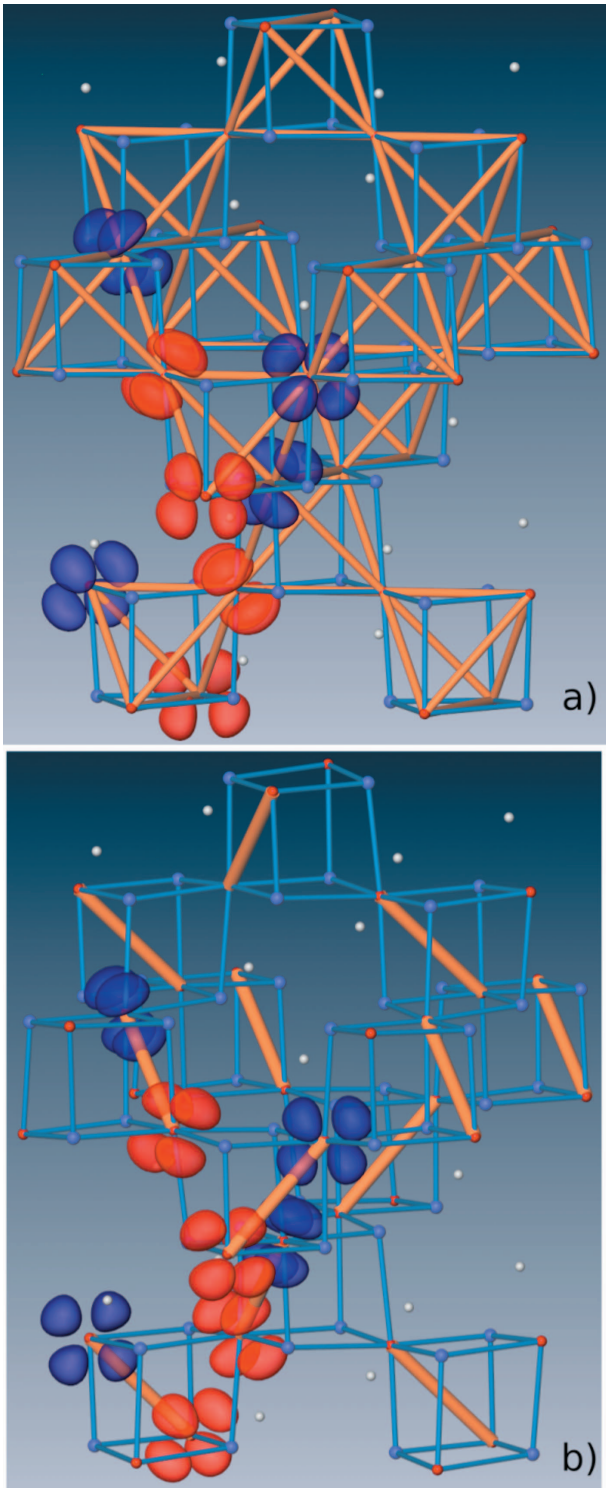


FIG. 3. (Color) Orbital ordering of  $\text{MgTi}_2\text{O}_4$  as obtained within LSDA+ $U$  ( $U=3$  eV) in the antiferropseudocubic (a, upper panel) and antiferrodimerized phase (b, lower panel). The red and blue colors denote the ground-state orbital with different ( $\uparrow, \downarrow$ ) spins.

According to LDA results for cubic  $\text{MgTi}_2\text{O}_4$  the occupation of the  $e'_g$  states is appreciably higher than that of the  $a_{1g}$  one. Already in LDA calculations for the dimerized phase, the degeneracy of the  $e'_g$  orbitals is lifted as a consequence of the local distortion of  $\text{TiO}_6$  octahedra and overall tetragonal symmetry. One of them (orange curve in Fig. 2) acquires XZ

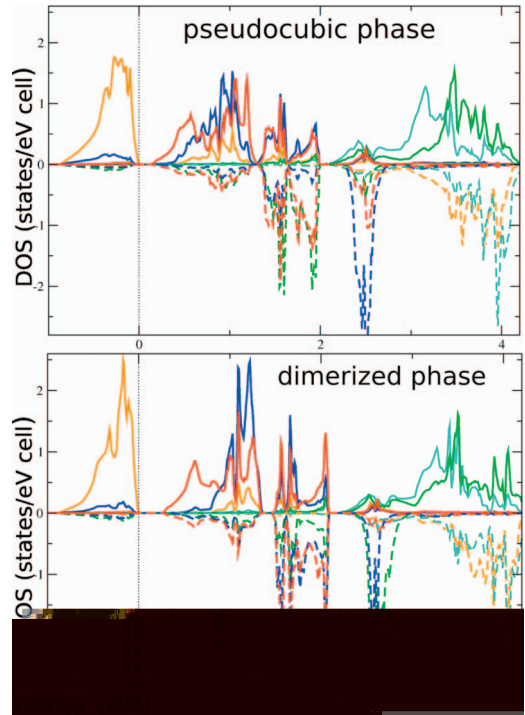


FIG. 4. (Color) LSDA+ $U$  orbital resolved DOS for  $U=3$  eV in the antiferropseudocubic phase (upper panel) and in the antiferrodimerized phase (lower panel) of  $\text{MgTi}_2\text{O}_4$ . Within dimers, DOS of different sites are mirror images with respect to spin space.

character and becomes more populated than the  $YZ$  one (blue). The  $XY$  orbital (red), originating from the  $a_{1g}$  state, forms a peak just above the Fermi level ( $E_F$ ), its occupation being less than that of the other two. This picture does not change much in the weak correlation regime ( $U \lesssim 3$  eV).

With increasing  $U$  ( $3 \text{ eV} \leq U \leq 5 \text{ eV}$ ) transfer of spectral weight significantly modifies the weakly correlated scenario

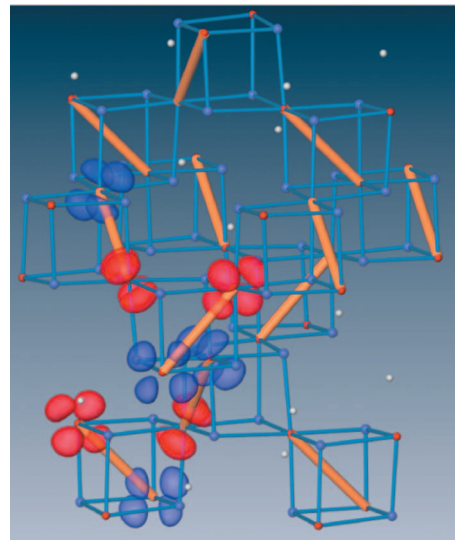


FIG. 5. (Color) Additional magnetically ordered LDA+ $U$  solution ( $U=3$  eV) with the same FOO as the ground-state solution, however with FM spin order in the  $a, b$  plane and AFM spin order along  $c$ . Red and blue colors denote the orbitals with different ( $\uparrow, \downarrow$ ) spins.

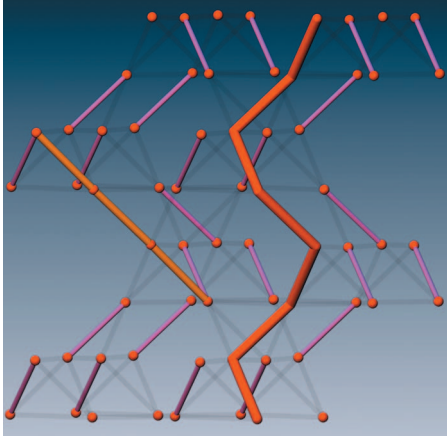


FIG. 6. (Color) ( $U=3$  eV). Ti-Ti shortest dimers are represented in mauve. Tetramers and spirals (only one representative is shown in orange and red, respectively) arise from distorting the pyrochlore lattice (black transparent bonds) from cubic to tetragonal. Only Ti atoms are displayed for clarity.

such that the  $XZ$  orbital is now almost half filled ( $n_{XZ} > 0.8$ ), whereas  $YZ$  and  $XY$  states are pushed toward the  $e_g$  bands, reducing the  $t_{2g}-e_g$  charge transfer gap. In this large  $U$  regime the overall electronic bandwidth is enhanced, accompanied by a reduction of the DOS near  $E_F$  and selection of a single orbital channel to form the insulating state. We observe a clear tendency toward a pseudogap formation in the  $XZ$  and  $YZ$  channels ( $U=5$  eV), while the  $XY$  orbitals are pushed to higher energies. This indicates OP as the precursor of the MIT. By further increasing  $U$  we obtain an insulating state at  $U=6$  eV. Our paramagnetic insulating solution is characterized by an almost half filled  $XZ$  band, with appreciable splitting between occupied bonding and unoccupied antibonding states.

The bonding-antibonding splitting observed at large  $U \geq 5$  eV (Fig. 2) aids the formation of the charge gap. The insulating state can be viewed as a consequence of strong hopping between the  $XZ$  orbitals along the short Ti-Ti bonds, leading to robust singlet character of these bonds (see discussion below) along the  $c$  axis. Thus, according to our results  $\text{MgTi}_2\text{O}_4$  undergoes an orbital-selective MIT,<sup>12</sup> which is caused by correlation-assisted orbital rehybridization.<sup>16</sup>

The changes in OO and crystal structure are shown in Fig. 1. Consistent with Ref. 9 ferro-orbital order (FOO) along the short Ti-Ti bonds, which stabilizes the molecular bond (orange) formation, starts to develop already for  $U \leq 3$  eV. The spiraling of the dimer bonds along the  $c$  axis is visible in Fig. 1. For  $U=3$  eV we obtain FOO, with the ground-state orbital pointing through bond's direction.

We now turn our attention to orbital, spin and charge responses in the magnetically ordered state. In Figs. 3 and 4 we display our LSDA+ $U$  ( $U=3$  eV) results for an idealized *pseudocubic* (upper panel) pyrochlore structure and the low- $T$  tetragonal structure (lower panel).<sup>7</sup>

In the idealized pseudocubic (PC) phase all atoms are arranged as in the high- $T$  cubic structure supplemented by a reduced ( $P4_12_12$ ) tetragonal space group. This combination of atomic arrangements and crystal symmetries allows for

the discovering of novel magnetic and orbital reorientations in the undistorted pyrochlore structure of  $\text{MgTi}_2\text{O}_4$ , which are in principle allowed in the vicinity of the MIT point.<sup>10</sup>

The orbital resolved DOS of the PC structure (Fig. 4) shows large OP and a small charge gap between the ground ( $XZ$ ) and the first excited  $XY$  orbital. Notice the dramatic rearrangement of the minority states of the ground-state orbital, which are shifted to energies above 3 eV. Within the tetragonal metric of the low- $T$  phase we find a similar evolution for the magnetically ordered electronic DOS as for the pseudocubic regime.

In the lower panel of Fig. 3 we display the ground-state OO in the distorted phase of  $\text{MgTi}_2\text{O}_4$ . The LSDA+ $U$  solution gives the same antiferromagnetic (AFM) arrangement of spins along the short Ti-Ti bonds and in the  $a, b$  plane of the pyrochlore lattice, as found for the PC structure. The lower panel of Fig. 3 shows, however, that the canting of the  $XZ$  orbitals away from the Ti-Ti bond plane becomes significantly smaller when the low- $T$  structural distortions are taken into account. Also, the average Ti-O distance in the  $XZ$  plane (2.068 Å) is appreciably larger than in the  $YZ$  (2.052 Å) and  $XY$  (2.041 Å) planes, which means that the occupation of the  $XZ$  state becomes energetically more favorable. This suggests a novel scenario for quasi-1D chains<sup>9</sup> in the strongly frustrated network of  $\text{MgTi}_2\text{O}_4$ , where the crystal structure itself gets modified by the onset of OO. The small changes in the atomic positions of the Ti ions shown in Fig. 3 additionally suggest that crystal structure transformations are coupled to the correlation-induced orbital reorientation.

Another magnetically ordered LSDA+ $U$  solution (Fig. 5) with the same FOO but FM spin order in the  $a, b$  plane and AFM one along the  $c$  direction can also be obtained for both the PC and dimerized structures. The order along the short Ti-Ti bonds remains FOO with AFM spin order, however, the Ti spins at the ends of intermediate Ti-Ti bonds with AFOO ( $XZ-YZ$ ) in the  $c$  direction are antiparallel. As a consequence, the total energy of this solution is higher than the ground-state solution shown in Fig. 3, in which the order along intermediate bonds is AFOO with FM spin order.

The dimerization of AFM spin chains and the formation of spin singlets located on short bonds explain the crystal structure of  $\text{MgTi}_2\text{O}_4$ , which can be seen as a collection of helices running along the  $c$  axis. This helix is formed by an alternation of short-long-short-long bonds as found in Ref. 7. As a consequence of the selective bond shortening superstructure features like tetramers can be recognized (Fig. 6).

The static calculations have provided evidence on the role of electronic correlation in the formation of the spin-singlet state. To further unravel the coupling between structural rearrangement and correlation-assisted OO, we have performed full structure relaxation in the correlated LDA+ $U$  potential. Starting from the cubic structure with pyrochlore sublattice, Parrinello-Rahman<sup>17</sup> (PR) structure relaxation<sup>18</sup> was performed. The Lagrangian formulation of PR allows for constant-pressure relaxation simulations, as variations in size and shape of the simulation box are allowed. This is typically used in connection with pressure-induced phase transitions. Here  $U$  is acting as some sort of “pressure” on the orbital channels, whose rehybridization brings structural changes about. To properly capture this effect it is thus im-

portant to dispose of a molecular dynamics setup allowing for unbiased geometry changes. For  $U=3$  eV structural lock-in into the tetragonal dimerized phase is achieved with selective shortening of a subset of bonds (*molecular dimers*) as displayed in Fig. 6. The role of local Coulomb interaction  $U$  as symmetry-reducing agent through selection of one orbital channel is apparent in the frame of the dynamic calculations. The found dimensional reduction selects thus a particular topological order among the various “degenerated valence bond configurations,” allowed in the quantum dimer framework of frustrated lattices,<sup>19</sup> in agreement with experiments.

### III. CONCLUSION

In conclusion, we have studied the ground-state orbital, charge, and magnetic properties of  $\text{MgTi}_2\text{O}_4$  using the LDA+ $U$  technique. Our results suggest an orbital-selective<sup>12</sup> picture for the metal-insulator transition of  $\text{MgTi}_2\text{O}_4$ , which is driven by large spectral weight transfer due to correlations

(via LDA+ $U$ ). This in turn introduces a new type of bonding-antibonding splitting near the Fermi energy, which is characterized by large orbital polarization of excited orbitals. Using the LSDA+ $U$  results we have computed the orbital order pattern in both high- $T$  pseudocubic and dimerized phase. The insulating low- $T$  phase is shown to be driven by electron correlations in concert with spin and orbital order. The existence of short Ti-Ti distances along the  $c$  axis follows as a consequence of spin dimerization on bonds (molecular dimers). Finally, consistent with x-ray diffraction experiments<sup>7</sup> the resulting superstructure features (tetramers, spirals) are shown to be carried by correlation over orbital order, explaining magnetic and structural properties of  $\text{MgTi}_2\text{O}_4$  in its low- $T$  insulating phase.

### ACKNOWLEDGMENTS

S.L. thanks the Swiss National Science Foundation for financial support. L.C. and H.R. acknowledge support from the Emmy Noether-Programm of the DFG. Computational time provided by ZIH, Dresden is acknowledged.

- 
- <sup>1</sup>Y. Taguchi, Y. Oohara, H. Yoshizawa, N. Nagaosa, and Y. Tokura, *Science* **291**, 2573 (2001); S. T. Bramwell and M. J. P. Gingras, *ibid.* **294**, 1495 (2001); P. G. Radaelli, Y. Horibe, M. J. Gutmann, H. Ishibashi, C. H. Chen, R. M. Ibberson, Y. Koyama, Y.-S. Hor, V. Kiryukhin, and S.-W. Cheong, *Nature (London)* **416**, 155 (2002); T. Suzuki, M. Katsumura, K. Taniguchi, T. Arima, and T. Katsufuji, *Phys. Rev. Lett.* **98**, 127203 (2007).
- <sup>2</sup>E. Verwey, *Nature (London)* **144**, 327 (1939).
- <sup>3</sup>M. Isobe and Y. Ueda, *J. Phys. Soc. Jpn.* **71**, 1848 (2002).
- <sup>4</sup>J. Zhou, G. Li, J. L. Luo, Y. C. Ma, Dan Wu, B. P. Zhu, Z. Tang, J. Shi, and N. L. Wang, *Phys. Rev. B* **74**, 245102 (2006).
- <sup>5</sup>H. D. Zhou and J. B. Goodenough, *Phys. Rev. B* **72**, 045118 (2005).
- <sup>6</sup>Z. V. Popović, G. De Marzi, M. J. Konstantinović, A. Cantarero, Z. Dohčević-Mitrović, M. Isobe, and Y. Ueda, *Phys. Rev. B* **68**, 224302 (2003).
- <sup>7</sup>M. Schmidt, W. Ratcliff, II, P. G. Radaelli, K. Refson, N. M. Harrison, and S. W. Cheong, *Phys. Rev. Lett.* **92**, 056402 (2004).
- <sup>8</sup>P. G. Radaelli, *New J. Phys.* **7**, 53 (2005).
- <sup>9</sup>D. I. Khomskii and T. Mizokawa, *Phys. Rev. Lett.* **94**, 156402 (2005).
- <sup>10</sup>S. Di Matteo, G. Jackeli, C. Lacroix, and N. B. Perkins, *Phys. Rev. Lett.* **93**, 077208 (2004); S. Di Matteo, G. Jackeli, and N. B. Perkins, *Phys. Rev. B* **72**, 024431 (2005); G. Jackeli, *J. Mol. Struct.* **838**, 220 (2007).
- <sup>11</sup>V. I. Anisimov, J. Zaanen, and O. K. Andersen, *Phys. Rev. B* **44**, 943 (1991).
- <sup>12</sup>V. I. Anisimov, I. A. Nekrasov, D. E. Kondakov, T. M. Rice, and M. Sigrist, *Eur. Phys. J. B* **25**, 191 (2002).
- <sup>13</sup>O. K. Andersen, *Phys. Rev. B* **12**, 3060 (1975).
- <sup>14</sup>In the tetragonal frame  $XY \sim d_{x^2-y^2}$ ,  $XZ \sim (d_{zx} \pm d_{yz})/\sqrt{2}$ , and  $YZ \sim (d_{zx} \mp d_{yz})/\sqrt{2}$ , where the sign reflects Ti-Ti bond orientation.
- <sup>15</sup>In the cubic frame  $a_{1g}$  and  $e'_g$  states can be written as  $d_{a_{1g}} = (d_{xy} + d_{yz} + d_{zx})/\sqrt{3}$ ,  $d_{1e'_g} = (2d_{xy} - d_{yz} - d_{zx})/\sqrt{6}$ ,  $d_{2e'_g} = (d_{yz} - d_{zx})/\sqrt{2}$ .
- <sup>16</sup>C. A. Marianetti, G. Kotliar, and G. Ceder, *Phys. Rev. Lett.* **92**, 196405 (2004).
- <sup>17</sup>M. Parrinello and A. Rahman, *Phys. Rev. Lett.* **45**, 1196 (1980).
- <sup>18</sup>S. Baroni, A. Dal Corso, S. de Gironcoli, P. Giannozzi, C. Cavazzoni, G. Ballabio, S. Scandolo, G. Chiarotti, P. Focher, A. Pasquarello, K. Laasonen, A. Trave, R. Car, N. Marzari, and A. Kokalj (<http://www.pwscf.org/>).
- <sup>19</sup>M. Levin and T. Senthil, *Phys. Rev. B* **70**, 220403(R) (2004).